

Cold-Source Measurements for Noise Figure Calculation in Spectrum Analyzers

N. Otegi, J.M. Collantes, M. Sayed¹

Electricity and Electronics Department, University of the Basque Country, Apdo. 644, 48080 Bilbao, Spain

Phone: +34-94-601-2464, Fax: +34-94-601-3071, Email: jmcollan@we.lc.ehu.es

¹Microwave & MillimeterWave Solutions, Santa Rosa, California, USA

Abstract — A detailed analysis of the suitability of *cold-source* based noise figure measurements in a spectrum analyzer is given in this paper. This technique presents some advantages in comparison to classical *Y-factor* techniques when dealing with problems related to device input match. A fully corrected noise figure calculation procedure, complemented with vector corrections and receiver noise calibration, is analyzed. For that, a noise calibration of the spectrum analyzer receiver, based upon analytical calculation, is given.

Index Terms — noise figure, noise measurements, cold-source, receiver noise calibration.

I. INTRODUCTION

Research and development in microwave instrumentation shows a growing tendency to integrate different types of measurements in a single system, in an attempt to optimize the device characterization process. For instance, most modern spectrum analyzers (SA) include noise figure calculation among their main features. In general this calculation is based on the well-known classical *Y-Factor* technique that makes use of two scalar power measurements, as in classical noise figure meters. This scalar *Y-factor* approach yields accurate results provided that device under test (DUT) is properly matched. When this is not the case, DUT mismatch can lead to significant systematic error in the calculation depending on device and setup characteristics. The noise measurements performed in a SA can be combined with vector measurements on a network analyzer in order to correct mismatch effects and improve accuracy in the noise figure calculation. However, when dealing with these mismatch corrections, *Y-factor* technique may not be the most suitable approach. Instead, *cold-source* technique, in which the device is measured with a source termination at only one temperature (room temperature), presents some advantages, particularly concerning errors coming from DUT input mismatch.

In this work, the suitability of *Y-factor* and *cold-source* techniques for mismatch error correction in noise figure calculation is analyzed. The bases of these techniques are well reported in the literature [1-4]. A procedure to perform fully-corrected noise figure measurements based on *cold-source* technique is given. This approach complements the scalar measurements of the SA with vector measurements. In

addition, a calibration method to obtain the four noise parameters of the SA is described since those parameters are essential to achieve an appropriate correction of the systematic errors associated to DUT output mismatch [5]. A measurement example of full-corrected noise figure measurements in a poorly matched device is given.

II. SYSTEMATIC ERRORS FROM DUT INPUT MISMATCH

The influence of mismatch effects at the input of the DUT on the final accuracy of the noise figure calculated from *Y-factor* and *cold-source* techniques is analyzed here. These input effects include mismatch between noise source and DUT, as well as changes in the noise source reflection coefficient between its cold and hot states. In order to properly focus on the errors associated to this input stage, any effect related to DUT output mismatch is eliminated from this analysis. In addition, second stage correction is also neglected for simplicity (it will be addressed in the next section when dealing with DUT output mismatch).

In the standard *Y-factor* technique, the noise figure of the DUT is computed from two noise powers (N_h , N_c) measured with the noise source at its hot and cold temperatures (T_h , T_c) respectively. Assuming that the cold temperature T_c is equal to the reference temperature $T_0 = 290$ K, the noise figure is obtained from:

$$F_{YF} \equiv \frac{(T_h/T_0 - 1)}{(N_h/N_c - 1)} \quad (1)$$

This expression relies on the basis that DUT noise figure does not change between the two noise power measurements. However, if the noise source reflection coefficient changes from cold to hot state, some variation in the DUT noise figure will actually occur, since the noise figure depends on the reflection coefficient connected at the input of the device. Therefore, (1) may not accurately lead to the desired noise figure. The effect on (1) of these noise source variations can be analyzed mathematically by means of an error term.

The error associated to this *Y-factor* technique can be defined as the difference between the computed F_{YF} and a reference value. Here, the actual noise figure of the DUT for the cold state of the noise source, $F(\Gamma_{sc})$, will be taken as the reference value.

$$e_{YF_IN} \equiv F_{YF} - F(\Gamma_{sc}) \quad (2)$$

It can be demonstrated that the error in (2) can be written as a function of DUT and setup parameters as in (3), shown at the bottom of this page. In (3), Γ_{sc} and Γ_{sh} are the noise source reflection coefficients corresponding to its cold and hot states, respectively, and $F(\Gamma_{sc})$, $F(\Gamma_{sh})$ are the DUT noise figures associated to these two states. Finally, s_{11} is the input S-parameter of the DUT.

It is clear from (3) that there is an error associated to the variation of the noise source reflection coefficient between its cold and hot state. It is important to note that the error is related to differences in the noise source reflection coefficient and not to mismatch between noise source and DUT. Indeed, this error is magnified as DUT input match worsens. On the contrary, regardless of the value of the reflection coefficient and input match, no error is obtained if the reflection coefficient of the noise source does not change from cold to hot state. That is, if $\Gamma_{sc} = \Gamma_{sh}$, then the error is null for any s_{11} :

$$e_{YF_IN}(\Gamma_{sc} = \Gamma_{sh}) = 0 \quad (4)$$

On the contrary, if the reflection coefficient of the noise source changes from cold to hot, error is present even for perfect input match of the DUT. In fact, if $s_{11} = 0$ the error can be expressed as:

$$e_{YF_IN}(s_{11} = 0) = \frac{\left(\frac{T_h}{T_0} - 1\right) F(\Gamma_{sc})}{\left(\frac{(1 - |\Gamma_{sh}|^2)}{(1 - |\Gamma_{sc}|^2)} F(\Gamma_{sh}) - F(\Gamma_{sc})\right) + \frac{(1 - |\Gamma_{sh}|^2)}{(1 - |\Gamma_{sc}|^2)} \left(\frac{T_h}{T_0} - 1\right)} - F(\Gamma_{sc}) \quad (5)$$

The effect of noise source variations on (1) can be reduced thanks to vector measurements, [1]. For that, a correction factor has to be applied to the measured hot noise power N_h :

$$N_{h_corr} \equiv N_h \frac{G_{av}(\Gamma_{sc})}{G_{av}(\Gamma_{sh})} \quad (6)$$

where $G_{av}(\Gamma_{sc})$ and $G_{av}(\Gamma_{sh})$ are, respectively, the DUT available gains for the cold and hot states of the noise source, computed from vector measurements. Introducing this term

instead of the scalar expression N_h , a vector corrected version of Y -factor can be obtained:

$$F_{YF_corr} \equiv \frac{(T_h/T_0 - 1)}{(N_{h_corr}/N_c - 1)} \quad (7)$$

and the corresponding error, defined as above, becomes:

$$e_{YF_corr_IN} = \frac{(T_h/T_0 - 1) F(\Gamma_{sc})}{(F(\Gamma_{sh}) - F(\Gamma_{sc})) + (T_h/T_0 - 1)} - F(\Gamma_{sc}) \quad (8)$$

Although all mismatch terms have disappeared from (8), the variation of the DUT noise figure from cold to hot measurement can still lead to an inaccurate result. Thus, the systematic error associated to noise source variations can not be fully removed from Y -factor technique since that would require, in addition to vector measurements, the knowledge of the DUT noise parameters, i.e. the knowledge of the noise figure itself.

On the other hand, the *cold-source* technique computes the noise figure from a single noise measurement N_c , with a source termination (Γ_{sc} as close to zero as possible) at room temperature, connected to the input of the DUT. Since the device is measured here at a unique noise source state, the errors associated to noise source variation are minimized, and can be fully eliminated, as it will be shown.

In order to compute the noise figure, the gain-bandwidth product of the receiver, kBG_{rec} , and the available gain of the DUT, $G_{av}(\Gamma_{sc})$, have to be previously determined. Again, assuming that the room temperature is equal to the reference temperature T_0 , the noise figure can be computed from (9).

$$F_{CS1} \equiv \frac{N_c}{T_0 kBG_{rec} G_{av}(\Gamma_{sc})} \quad (9)$$

where perfect output match is considered and the second stage correction has been neglected as in the Y -factor case for simplicity purposes (second stage correction will be addressed in the next section).

The DUT available gain is computed from vector measurements. The kBG_{rec} term is obtained from two noise power measurements, N_{c_rec} and N_{h_rec} , carried out with the noise source directly connected to the receiver input:

$$e_{YF_IN} = \left\{ \frac{\frac{(1 - |\Gamma_{sc}|^2)}{|1 - \Gamma_{sc}s_{11}|^2} \left(\frac{T_h}{T_0} - 1\right) F(\Gamma_{sc})}{\left(\frac{(1 - |\Gamma_{sh}|^2)}{|1 - \Gamma_{sh}s_{11}|^2} F(\Gamma_{sh}) - \frac{(1 - |\Gamma_{sc}|^2)}{|1 - \Gamma_{sc}s_{11}|^2} F(\Gamma_{sc})\right) + \frac{(1 - |\Gamma_{sh}|^2)}{|1 - \Gamma_{sh}s_{11}|^2} \left(\frac{T_h}{T_0} - 1\right)} - F(\Gamma_{sc}) \right\} \quad (3)$$

$$kBG_{rec} \equiv \frac{N_{h_rec} - N_{c_rec}}{T_h - T_0} \quad (10)$$

Again, the error associated to this *cold-source* technique is defined as the difference between the F_{CS1} term computed from (9) and a reference value. In this case, the reference value will be the actual noise figure of the DUT for the source termination $F(\Gamma_{sc})$:

$$e_{CS_IN} \equiv F_{CS1} - F(\Gamma_{sc}) \quad (11)$$

As in the previous case, the error term (11) can be expressed as a function of the setup parameters:

$$e_{CS_IN} = \frac{F(\Gamma_{sc})}{(T_2 - T_1)/(T_h - T_0)} - F(\Gamma_{sc}) \quad (12)$$

where

$$T_2 = MM(\Gamma_{sh})(T_0 F_{rec}(\Gamma_{sh}) + (T_h - T_0)) \quad (13)$$

$$T_1 = MM(\Gamma_{sc})T_0 F_{rec}(\Gamma_{sc}) \quad (14)$$

$F_{rec}(\Gamma_{sc})$, $F_{rec}(\Gamma_{sh})$ are the receiver noise figures for the cold and hot states of the noise source, respectively. MM is a mismatch term between the noise source and the receiver:

$$MM(\Gamma) \equiv \frac{1 - |\Gamma|^2}{|1 - s_{11_rec}\Gamma|^2} \quad (15)$$

with s_{11_rec} the input S-parameter of the receiver.

It is important to note that, in the *cold-source* case, variations in the noise source reflection coefficient from hot to cold state only affect the receiver, since the DUT is measured at a unique noise source state. This effect can be corrected if the noise parameters of the receiver are known. However, corrections do not involve the noise parameters of the DUT, which are obviously unknown, as in the case of *Y-factor* technique. As a consequence, the systematic error given by (11) can be fully eliminated with vector measurements, provided that the noise parameters of the receiver are known. Indeed, the kBG_{rec} term can be corrected to include noise source variations:

$$kBG_{rec_corr} \equiv \frac{N_{h_rec} - N_{c_rec}}{T_2 - T_1} \quad (16)$$

With this term (16) a corrected *cold-source* expression, where the effect of noise source variations has been fully eliminated, can be computed:

$$F_{CS1_corr} \equiv \frac{N_c}{T_0 kBG_{rec_corr} G_{av}(\Gamma_{sc})} \quad (17)$$

$$e_{CS_corr_IN} \equiv F_{CS1_corr} - F(\Gamma_{sc}) = 0 \quad (18)$$

Actually, due to practical noise and match characteristics of the receivers, ignoring its noise parameters leads to little error as far as noise source variation is concerned.

All the above issues can be widely analyzed with the help of a simulation program specifically developed for the analysis of systematic error and uncertainty in noise figure measurements [6]. Here some examples will be given for illustration purposes. For these examples same measurement setup, i.e. noise source and noise receiver, as in [7] is chosen. The above *Y-factor* and *cold-source* formulations, (1) and (9) respectively, are applied to two general purpose amplifiers, *DUT1* and *DUT2*, with different noise characteristics. The considered S-parameters for both amplifiers are: $|S_{21}| = 40$ dB, $S_{11} = \text{variable} \angle 0^\circ$, $S_{22} = 0 \angle 0^\circ$ (values consistent with the approximations made for the prior analysis are taken). *DUT1* noise parameters: $F_{min} = 5$ dB, $R_n = 50 \Omega$, $\Gamma_{opt} = 0.05 \angle 0^\circ$; *DUT2* noise parameters: $F_{min} = 5$ dB, $R_n = 50 \Omega$, $\Gamma_{opt} = 0.65 \angle 180^\circ$. The systematic error given by both techniques is analyzed as a function of DUT input match.

Fig. 1 shows the results obtained for *DUT1*. As expected from the previous analysis, the error is negligible for *cold-source* technique, since the noise source variation only affects the receiver. If the error were higher, it could be corrected as shown in (17), which would require the noise parameters of the receiver. Besides, *Y-factor* presents an increasing error as input match worsens. For good input match, this error is not really significant, due to the noise characteristics of *DUT1*.

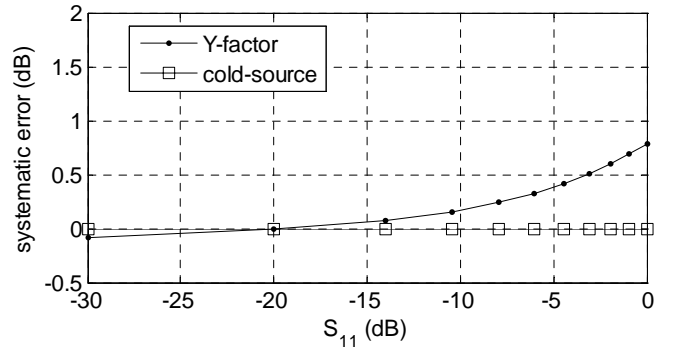


Fig. 1. Systematic error obtained with *Y-factor*, (1), and *cold-source*, (9), techniques for *DUT1*

Results for *DUT2* are given in Fig. 2. The error for *cold-source* technique is negligible again, since it does not depend on DUT noise characteristics. Besides, the error given by *Y-factor* is higher than in the previous case, because of the noise properties of this DUT. Significant error even for perfect input match is obtained, which is consistent with (5).

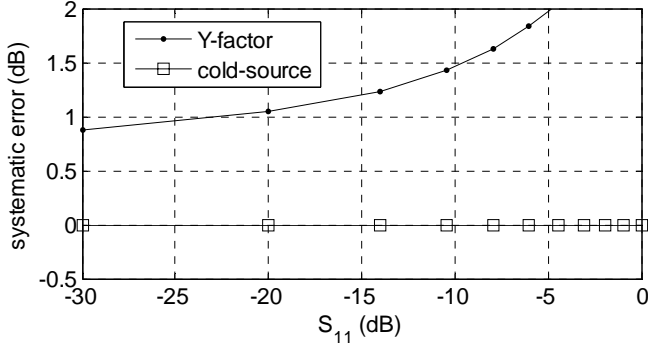


Fig. 2. Systematic error obtained with *Y-factor*, (1), and *cold-source*, (9), techniques for *DUT2*

Finally, the effect of vector corrections on *Y-factor* methodology for both devices will be analyzed. For that the mismatch correction (6) is applied. While the error is eliminated for *DUT1*, the considerable difference in *DUT2* noise figure from cold to hot measurement causes a significant constant error, according to (8).

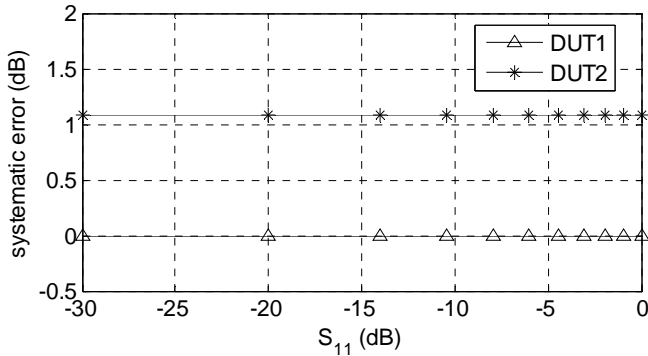


Fig. 3. Systematic error obtained with *Y-factor* technique (7), which includes vector corrections to minimize the error associated to $\Gamma_{s_c} \neq \Gamma_{s_h}$

III. SYSTEMATIC ERRORS FROM DUT OUTPUT MISMATCH

As it has been shown in the previous section, *cold-source* technique is specially adapted for eliminating errors associated to mismatch effects at DUT input. However, systematic effects related to output match can significantly degrade the final accuracy of noise figure measurements for low gain devices, in a similar manner than occurs for the *Y-factor* technique [5].

In this section variations on the noise source are neglected and, therefore, $\Gamma_{sh} = \Gamma_{sc}$ is assumed. This means that receiver noise figure will not change within the calibration process and only the effect of differences from calibration to measurement stage is analyzed.

In order to analyze the errors related to output stage, the standard *cold-source* formulation is considered:

$$F_{CS2} \equiv \frac{N_c - N_{c_rec}}{T_0 k B G_{rec} G_{av}(\Gamma_{sc}) MM(\Gamma_{out})} + \frac{1}{G_{av}(\Gamma_{sc})} \quad (19)$$

which adds to (9) a correction for eliminating the receiver noise and a mismatch term MM for taking into account the mismatch between DUT and receiver. The noise power N_{c_rec} is the noise generated by the receiver when the noise source is directly connected, in the cold state Γ_{sc} , to it. However, the noise generated by the receiver in the measurement stage actually depends on the DUT output reflection coefficient Γ_{out} and not on the noise source reflection coefficient Γ_{sc} . Neglecting the dependence of the receiver noise on its input reflection coefficient can lead to significant error in the computed noise figure.

An error expression can be defined as in section II for the computed noise figure F_{CS2} :

$$e_{CS_OUT} \equiv F_{CS2} - F(\Gamma_{sc}) \quad (20)$$

This error term (20) can be written as a function of the receiver noise figure through some simple algebraic operations:

$$e_{CS_OUT} = \frac{1}{G_{av}(\Gamma_s)} \left(F_{rec}(\Gamma_{out}) - \frac{MM(\Gamma_s)}{MM(\Gamma_{out})} F_{rec}(\Gamma_s) \right) \quad (21)$$

As expected, the error is inversely proportional to DUT gain and increases as Γ_{out} diverges from Γ_s .

It should be remarked that this methodology takes into account the mismatch between DUT and receiver through the $MM(\Gamma_{out})$ term. However, the result may still be inaccurate for poorly matched devices, due to the lack of noise calibration of the receiver. If the receiver noise parameters are obtained, its actual noise figure corresponding to measurement stage can be calculated. Then, the corrected noise figure is computed from (22), which eliminates the error for any Γ_{out} .

$$F_{CS2_corr} \equiv \frac{N_c}{T_0 k B G_{rec} G_{av}(\Gamma_s) MM(\Gamma_{out})} - \frac{F_{rec}(\Gamma_{out}) - 1}{G_{av}(\Gamma_s)} \quad (22)$$

$$e_{CS_corr_OUT} \equiv F_{CS2_corr} - F(\Gamma_{sc}) = 0 \quad (23)$$

As in section II, a case example is studied by means of simulation. For that, a mixer, *DUT3*, with the following characteristics is chosen: $S_{11} = 0.43 \angle 0^\circ$, $S_{22} = \text{variable} \angle 110^\circ$, $|S_{21}| = 2$ dB, $F \approx 7$ dB, is taken. Although mixer noise figure characterization is a complex task affected by many systematic effects, in this example only the error arising from an inadequate second stage correction is analyzed. The systematic errors given by the standard and the corrected *cold-source* methodologies, (19) and (22) respectively, are shown versus DUT output match in Fig. 4.

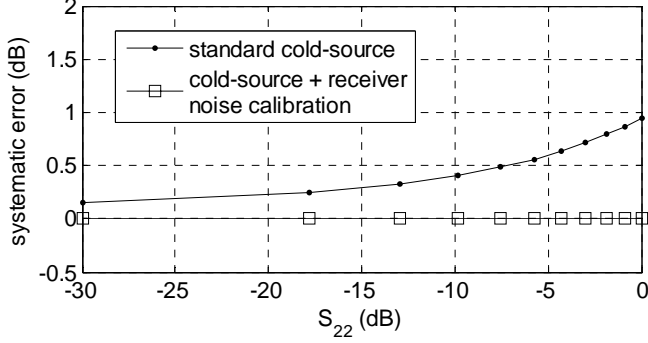


Fig. 4. Systematic error obtained with standard *cold-source* technique (19) and *cold-source* technique with receiver noise calibration (22) for DUT3

Fig. 4 shows a considerable error as mixer output match worsens, as could be expected from its low gain. This result confirms that vector corrections are not sufficient for properly dealing with output match problems. Thus, the knowledge of the receiver noise parameters is essential for accurately measuring the noise figure of low gain poorly matched devices.

IV. NOISE CALIBRATION OF THE SA

As it has been shown in the previous section, for the mismatch corrections to be rigorous and efficient, a complete noise calibration of the system receiver is essential. For that end, a noise calibration procedure, initially developed for vector network analyzers [8], has been adapted to the SA, with the aim of simplifying the obtaining of the four noise parameters as much as possible. The bases of this procedure are detailed in the following paragraphs.

Let us consider a system composed of the DUT and the noise receiver. The DUT noise figure can be obtained from the Friis formula for cascaded systems as:

$$F_{DUT} = F_{sys} - \frac{F_{rec}(\Gamma_{out}) - 1}{G_{av}(\Gamma_{out})} \quad (24)$$

where F_{sys} is the global noise figure of the cascaded system. The dependence of the receiver noise figure F_{rec} on the DUT output reflection coefficient Γ_{out} is usually given by means of noise parameters F_{min} , R_n and Γ_{opt} , as:

$$F_{rec}(\Gamma_{out}) = F_{min} + 4 \frac{R_n}{Z_0} \frac{|\Gamma_{out} - \Gamma_{opt}|^2}{|1 + \Gamma_{opt}|^2 (1 - |\Gamma_{out}|^2)} \quad (25)$$

Using straightforward algebra, the second stage correction term can be rewritten as:

$$\Delta_2 = \frac{F_{rec}(\Gamma_{out}) - 1}{G_{av}(\Gamma_{out})} = \frac{|1 - s_{11}\Gamma_s|^2}{(1 - |\Gamma_s|^2)|s_{21}|^2} I(\Gamma_{out}) \quad (26)$$

where Γ_s is the reflection coefficient of the noise source and s_{ij} are the DUT S-parameters. Therefore, the $I(\Gamma_{out})$ term compresses all the dependence on Γ_{out} of the second stage correction:

$$I = C_1 + C_2/|\Gamma_{out}|^2 + C_3/|\Gamma_{out}| \cos(\angle\Gamma_{out} + C_4) \quad (27)$$

being $\{C_1, C_2, C_3, C_4\}$ four noise parameters, equivalent to the $\{F_{min}, R_n, \Gamma_{opt}\}$ set, that completely characterize the noise properties of the receiver as a function of Γ_{out} .

$$C_1 = F_{min} - 1 + \frac{4R_n}{Z_0} \frac{|\Gamma_{opt}|^2}{|1 + \Gamma_{opt}|^2} \quad (28)$$

$$C_2 = \frac{4R_n}{Z_0} - (F_{min} - 1) \quad (29)$$

$$C_3 = -2 \frac{4R_n}{Z_0} \frac{|\Gamma_{opt}|}{|1 + \Gamma_{opt}|^2} \quad (30)$$

$$C_4 = -\angle\Gamma_{opt} \quad (31)$$

It can be easily deduced that the noise generated by a passive termination with a reflection coefficient Γ_i , connected to the receiver at the reference temperature T_0 , is related to I as:

$$I = N_i \frac{|1 - \Gamma_i s_{11rec}|^2}{T_0 K B G_{rec}} - (1 - |\Gamma_i|^2) \quad (32)$$

Therefore, obtaining $I(\Gamma_i)$ for four known terminations allows the determination of the four C_i parameters by analytically solving a set of four linear equations with four unknowns. For that end, (27) must be rewritten as:

$$I = C_1 + C_2/|\Gamma_{out}|^2 + D_3/|\Gamma_{out}| \cos(\angle\Gamma_{out}) - D_4/|\Gamma_{out}| \sin(\angle\Gamma_{out}) \quad (33)$$

where,

$$D_3 = C_3 \cos C_4 \Rightarrow \text{tg} C_4 = D_4 / D_3 \quad (34)$$

$$D_4 = C_3 \sin C_4 \Rightarrow C_3 = \pm \sqrt{D_3^2 + D_4^2} \quad (35)$$

There is a sign uncertainty in the above equations that is easily overcome by taking into account that, from (30), C_3 is negative. Expression (33) can be considerably simplified if a matched load, $\Gamma \approx 0$, or a highly reflective load, $|\Gamma| \approx 1$, are considered. This suggests that a reasonable set of standards could be composed of a matched load and three reflective terminations. Three out of these four standards can be found in a typical SOLT calibration kit for S-parameters of a vector network analyzer: a matched load, an open circuit and a short circuit; the fourth standard can be built adding a length of

transmission line to any of the two reflective loads. It is important to remark that the open circuit and the short circuit will maintain approximately a 180° phase difference in the whole measuring range. However, the third reflective standard can approximate to any of them as the frequency varies, this implying an ill-conditioned phase distribution that would degrade the analytical calculation of (32), [9]. Therefore, the length of the transmission line should be carefully chosen in order to avoid an ill-conditioned phase distribution. Nevertheless, in a broadband measurement these ill-conditioned distributions are unavoidable for certain frequencies. For these problematic ranges the standard or the transmission line length should be changed. Indeed, an additional standard could be included and then, the best phase condition chosen.

In order to validate in a SA this receiver noise calibration technique, it has been applied to the correction of a passive, highly mismatched DUT (see Fig. 5). This kind of device provides a good reference because, on the one hand, its actual noise figure can be analytically computed from S-parameters measurements ($F=1/G_{av}$); on the other hand, it represents a worst case situation since having losses instead of gain magnifies output mismatch effects.

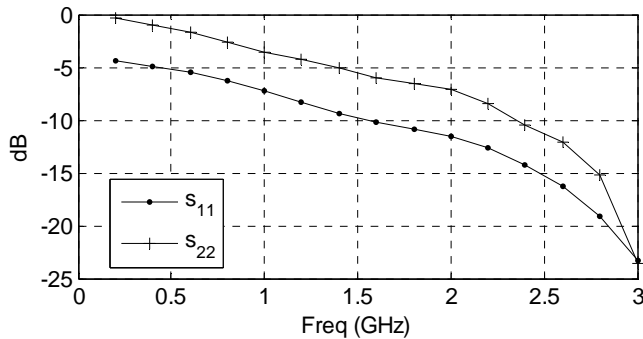


Fig. 5. DUT s_{11} and s_{22} in the 200 MHz-3 GHz range

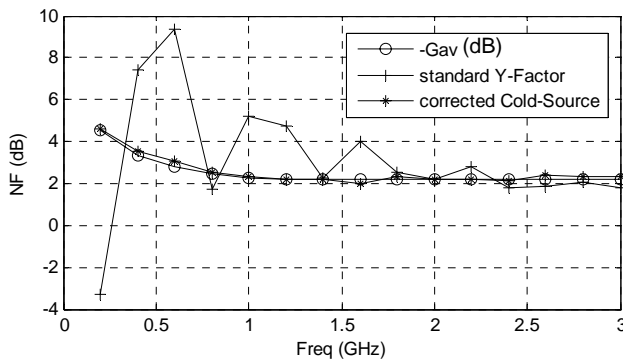


Fig. 6. Noise figure measurement results for a passive mismatched DUT in the 200 MHz-3 GHz range

The measurements have been performed on a PSA E4460A with noise figure measurement capability, in the 200 MHz-3 GHz band. The fully corrected cold source

technique given by (22) has been applied. The obtained result, shown in Fig. 6, has been compared to standard Y-factor technique (1) computed by the SA. Fig. 6 shows that the calibrated noise figure measurements provide very good results, confirming the suitability of the analytical calibration procedure for the SA. In contrast, the result given by Y-factor presents significant errors due to the device characteristics, the lack of a receiver noise calibration and mismatch correction terms.

VI. CONCLUSION

A vector-corrected *cold-source* methodology for noise figure measurements in a SA has been presented. *Cold-source* based methodologies minimize systematic effects from input stage and errors related to output are eliminated in the present approach thanks to mismatch corrections and receiver noise calibration.

ACKNOWLEDGEMENT

The authors wish to acknowledge Agilent Technologies for their support. This work has been funded by Spanish Commission of Science and Technology (TIC2003-04453).

REFERENCES

- [1] D. Vondran, "Noise Figure Measurement: Corrections related to match and Gain," *Microwave Journal*, March 1999, pp. 22-38
- [2] R. Meierer, C. Tsironis, "An On-Wafer Noise Parameter Measurement Technique with Automatic Receiver Calibration," *Microwave Journal*, March 1995, pp. 22-37.
- [3] V. Adamian, A. Uhlir, "A Novel Procedure for Receiver Noise Characterization," *IEEE Trans. on Instruments & measurements*, Vol. 22, No. 2, June 1973, pp.181-182.
- [4] "Fundamentals of RF and Microwave Noise Figure measurements," Agilent Application Note 57-1
- [5] J. M. Collantes, R.D. Pollard, M. Sayed, "Effects of DUT Mismatch on the Noise Figure Characterization: A Comparative Analysis of Two Y-Factor Techniques," *IEEE Trans. Inst& Meas*, vol. 51, no. 6, December 2002, pp. 1150-1156.
- [6] N. Otegi, J. M. Collantes, M. Sayed, "Uncertainty Estimation in Noise Figure Measurements at Microwave Frequencies," *IEEE International Workshop on Advanced Methods for Uncertainty Estimation in Measurements*, Niagara Falls, Ontario, Canada, pp. 84-89.
- [7] N. Otegi, J. M. Collantes, M. Sayed, "Statistical Analysis of Accuracy in Noise Figure Measurements," *66th ARFTG Conference Digest*, December 2005.
- [8] N. Otegi, J. M. Collantes, M. Sayed, "Calibrated Noise Figure Measurements in Vector Network Analyser," *Electronic Letters*, vol. 41, Issue 18, September 2005, pp. 999-1000
- [9] M. De Dominicis, F. Giannini, E. Limiti, G. Saggio: "A novel impedance pattern for fast noise measurements," *IEEE Trans. Instrum. Meas.*, 2002, 51, (3), pp. 560-564